J. Fluid Mech. (1979), *vol.* 90, *part* 3, *pp.* 449–463
Printed in Great Britain

The effects of rotation on salt fingers

By RAYMOND W. SCHMITT† AND RICHARD B. LAMBERT‡
Graduate School of Oceanography, University of Rhode Island, Kingston

(Received 21 July 1976 and in revised form 18 November 1977)

The effects of rotation on a salt-fingering interface between two mixed layers are studied experimentally. It is found that rotation causes an interface to thicken more rapidly than it does in the corresponding non-rotating experiment. In order to interpret this result, the collective-instability model of Stern (1969, 1975) is extended to include the Coriolis effect and the neutral-stability condition is derived. Rotation stabilizes the fingers, the degree of stabilization being dependent on the wavenumber of the perturbation. By assuming equal fluxes in the rotating and non-rotating experiments, the interface thickness data are found to be consistent with the extended collective-instability model.

1. Introduction

Convection is possible in a stably stratified fluid when the distribution of either heat or salt is gravitationally unstable and the overall stability is maintained by a stable distribution of the other component. When the salinity gradient is destabilizing, characteristically long narrow cells, which are called salt fingers, are generated (Stern 1960). Heat diffuses 100 times faster than dissolved salts in water, and the fingers are driven by the faster lateral diffusion of heat from one finger to the next. This allows the release of the potential energy stored in the salt gradient, resulting in a net downward density flux. Fingers can also be formed using solutes of only slightly different diffusivities, such as sugar and salt, in which case the diffusion coefficient of salt is only a factor of three greater than the diffusion coefficient of sugar (Stern & Turner 1969; Shirtcliffe & Turner 1970; Lambert & Demenkow 1972).

Fingers can have a rather large vertical extent, reaching throughout a region of uniform vertical gradients. However fingers can also be limited to thin, strongly stratified interfaces and can coexist with turbulent mixed regions above and below (Turner 1967; Turner & Chen 1974). Stern & Turner (1969) were able to initiate a series of layers and interfaces by imposing an excess flux of the slower diffusing substance S on a stable uniform gradient of the faster diffusing substance T. Such laboratory experiments have led many investigators to identify salt fingering as the driving mechanism for the maintenance of the 'thermohaline staircase' observed beneath the intrusion of warm salty Mediterranean water into the colder fresher Atlantic (Tait & Howe 1968). Williams (1975) has observed optical images of salt fingers on such stratified interfaces in the ocean, which adds to the evidence for this hypothesis. Lambert & Sturges (1977) have shown that fingering at interfaces transports enough

† Present address: Woods Hole Oceanographic Institution, Woods Hole, Massachusetts 02543.
‡ Present address: Science Applications Inc., 8400 Westpark Drive, McLean, Virginia 22101.

salt to be important in the large-scale salt budget of the main thermocline in the northeast Caribbean Sea.

A layer–interface system in the laboratory is fairly long lasting, apparently in a quasi-steady state. The net density flux through the finger interface drives the convection in the larger layers; this in turn appears to limit the vertical extent of the fingers, which are swept away by, and contribute to, the convective elements in the mixed layer. The only theory which treats a mechanism by which salt fingers may contribute to a larger-scale motion is the collective-instability model of Stern (1969, 1975).

Stern (1975) examined the stability of a field of fingers perturbed by a large-scale internal wave (wavelength > finger width) that produces convergence of the net density flux. Density anomalies so produced can cause the wave perturbation to grow if the net density flux exceeds the mean density gradient scaled in terms of the kinematic viscosity:

$$(\beta F_S - \alpha F_T)/\nu(\alpha \bar{T}_z - \beta \bar{S}_z) > 1, \tag{1.1}$$

where βF_S and αF_T are the magnitudes of the density fluxes due to S and T, respectively, $\beta \bar{S}_z$ and $\alpha \bar{T}_z$ are their separate contributions to the density gradient and ν is the kinematic viscosity. Stern (1969) derived the form appropriate for heat–salt fingers: $\beta F_S / \nu \alpha \bar{T}_z > 2$. He neglected the salinity gradient and assumed a constant flux ratio (suggested by the results of Turner 1967). Linden (1973) was able to show approximate agreement with this relation for laboratory measurements on a heat–solute system, but found the ratio to be a function of $\beta \Delta S / \alpha \Delta T$, where $\beta \Delta S$ and $\alpha \Delta T$ are the density differences due to the changes in S and T across the interface (Stern 1976). Lambert & Demenkow (1972) found that the non-dimensional group (1.1) was a constant, but that the critical value was much smaller than 1 for sugar–salt fingers. Whether this remains true as $\beta \Delta S / \alpha \Delta T \to 1$ is uncertain, but we expect the physics of the phenomenon to remain valid even if the numerical value of the non-dimensional group (1.1) is some function of $\beta \Delta S / \alpha \Delta T$ and K_T / K_S.

To explore further the properties of fingering interfaces we have performed some simple experiments with sugar–salt fingers on a rotating table. The results of these experiments are related to the collective-instability model by extending the analysis of Stern (1975) to include the Coriolis effect. The rotational constraint removes a degeneracy in that the two horizontal-component equations are no longer decoupled and a dependency on the wavenumber of the instability is found.

We present the observations in § 2 and the analysis in § 3. In § 4 we attempt to interpret the experiments in terms of the model. We feel that the observations are interesting in their own right but also provide support for the collective-instability mechanism, which has been incorporated in several theoretical studies of salt fingers (Lambert & Demenkow 1972; Stern 1976).

2. The experiments

Salt fingers on an interface were generated in a Plexiglas tank (26·9 × 10·3 × 24·7 cm deep) by introducing a 12 cm layer of sugar solution over a 12 cm layer of slightly denser salt solution. The thickness of the finger interface slowly increased with time as the solutes were transported across the interface, decreasing the concentration

Experiment	$\alpha\Delta T_0$	$\beta\Delta S_0$	ω (s $^{-1}$)	$\overline{h_r/h_0}$	n
$B1$	0·100	0·090	0	–	
$B2$	0·100	0·090	0·707	$1{\cdot}14 \pm 0{\cdot}06$	17
$A3$	0·100	0·090	0·966	$1{\cdot}30 + 0{\cdot}05$	13
$B3$	0·100	0·090	1·382	$1{\cdot}35 \pm 0{\cdot}07$	17
$C1$	0·100	0·095	0		–
$C2$	0·100	0·095	1·381	$1{\cdot}39 \pm 0{\cdot}08$	19

TABLE 1. Initial density conditions and angular velocities of rotation for the experiments. $\overline{h_r/h_0}$ is the average value of the ratio of the interfacial thicknesses in the rotating experiments to that in the non-rotating experiment with the same initial $\alpha\Delta T$ and $\beta\Delta S$. n is the number of photograph pairs (h_r, h_0) used in forming the average.

difference between the upper and lower reservoirs. The interface thickness was made visible by a horizontal shadowgraph technique (Shirtcliffe & Turner 1970). The shadowgraphs were photographed by a motor-driven camera mounted on the rotating table, and the growth of the interface was measured from the photographs (see figure 1, plate 1).

The solutions were prepared from distilled degassed water, with the initial densities measured with a hydrometer accurate to $\pm 0{\cdot}0005\,\mathrm{g/cm^3}$. The initial density of the salt solution was $\rho = 1{\cdot}100\,\mathrm{g/cm^3}$ for all experiments. The initial density of the sugar solution was varied, as was the rotation rate; the conditions of the several experiments are listed in table 1.

In the rotating experiments, the salt water was spun up before the sugar solution was introduced from a tank on the table, to avoid mixing of the two solutions during spin-up. The table was carefully levelled so that its axis was within a minute of the vertical, to avoid 'tidal' effects. The rotational period was measured by an electronic counter connected to a micro-switch on the table.

Photographs were taken at regular intervals (15 or 30 min) after the initiation of the pouring of the sugar solution. Samples of the photographs are shown in figure 1. The major difference between the rotating and non-rotating experiments is in the thickness of the interface. For the same initial conditions the rotating finger interface is thicker than the stationary one at the same elapsed time. The change in interface thickness h is shown quantitatively in figures 2 and 3, where h has been plotted as a function of time for both sets of experiments. Rotating interfaces are consistently found to be thicker than non-rotating interfaces, an increasing rotation rate giving a larger change in h (figure 2). There is also somewhat less vertical alignment of the fingers in the rotating case, fingers sometimes appearing to twist about one another, especially near the edges of the finger interface.

It is possible to interpret the increase in h in terms of the collective-instability relation. By approximating the gradients $\alpha\bar{T}_z$ and $\beta\bar{S}_z$ as $\sim\alpha\Delta T/h$ and $\beta\Delta S/h$, where $\alpha\Delta T$ and $\beta\Delta S$ are the density increments across the interface due to T and S, we may write the instability condition (1.1) in finite-difference form:

$$(\beta F_S - \alpha F_T)\,h/\nu(\alpha\Delta T - \beta\Delta S) > (1). \tag{2.1}$$

One interpretation is that, if this relation remains close to an equality, the interface may be considered self-limiting; that is, an increase in h would cause the fingers to

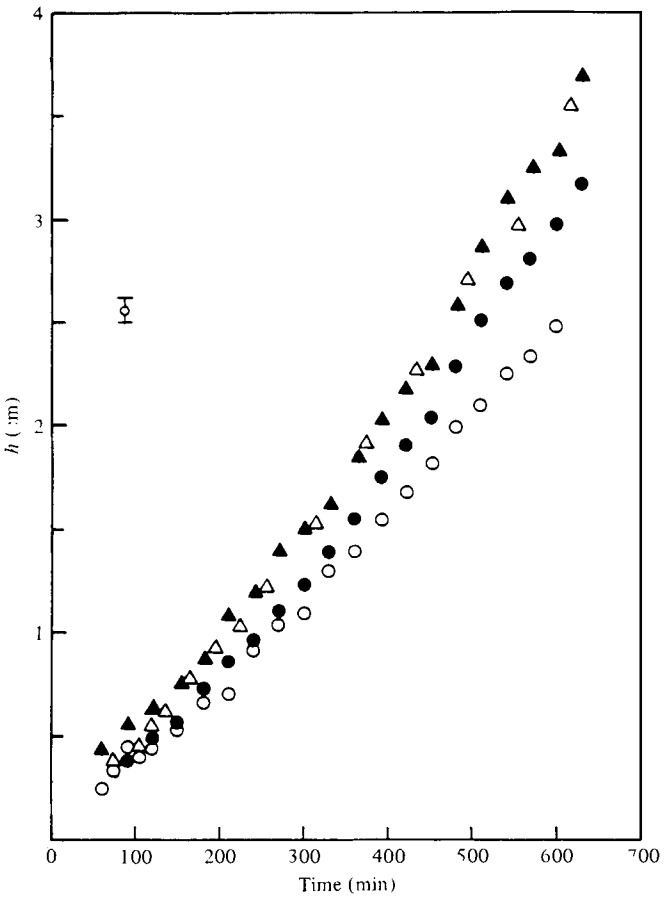

FIGURE 2. h, the thickness of the fingering interface, as measured from photographs taken at regular intervals in two-layer sugar–salt experiments with initial conditions $\alpha\Delta T_0 = 0{\cdot}10$, $\beta\Delta S_0 = 0{\cdot}09$ and various angular velocities. The uncertainty in h is $\pm 0{\cdot}5$ mm. , $\omega = 0$; ●, $\omega = 0{\cdot}707\,\mathrm{s}^{-1}$; △, ω $0{\cdot}966\,\mathrm{s}^{-1}$; ▲, ω $1{\cdot}38\,\mathrm{s}^{-1}$.

become unstable, the resulting turbulence then thinning the interface back to marginal stability. We may thus interpret the thicker finger interface under rotation as being due to a stabilizing effect of the rotation. We shall later show that the quantity on the right of (2.1) increases when rotation is added to the collective-instability model, thus allowing larger values of h at marginal stability.

Solute concentrations, which would be required for a complete comparison of the rotating and non-rotating regimes, were not measured during the experiments, but for one pair of experiments the index of refraction of the upper layer was checked at the ends of the runs and found to be the same in the rotating and non-rotating cases. We might expect that the fluxes of sugar and salt should be nearly the same in both cases because the flux depends primarily on $(\beta\Delta S)^{\frac{4}{3}}$; assuming equal fluxes allows us to make at least a first-order comparison between theory and experiment. Under this assumption a good measure of the stabilizing effect of rotation is the ratio h_r/h_0 of the height of the rotating interface to the height of the non-rotating interface.

A mean value of h_r/h_0 was estimated for each rotating experiment by averaging

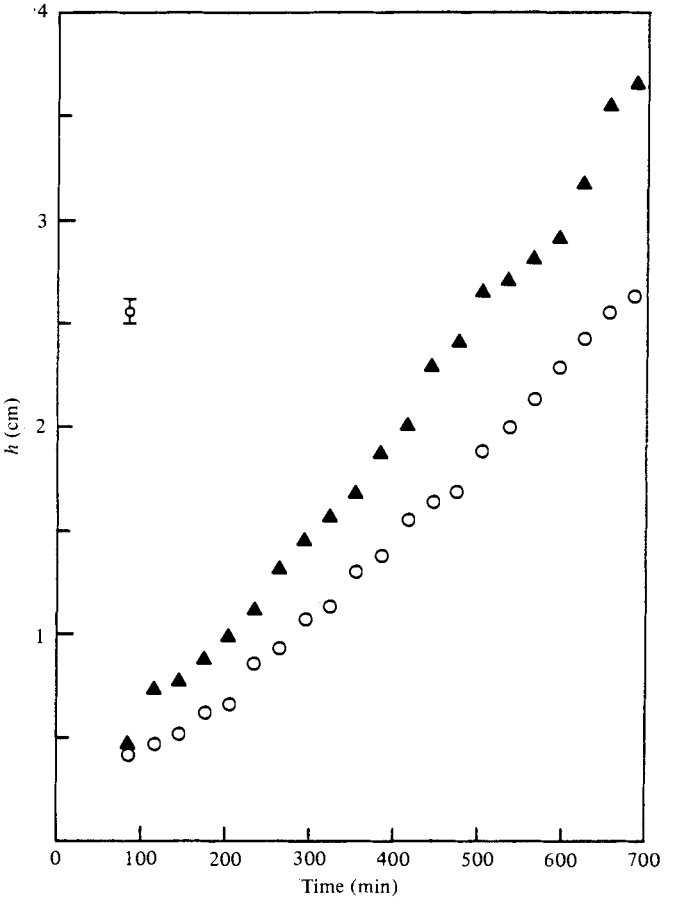

FIGURE 3. h as a function of time with initial conditions $\alpha\Delta T_0 = 0{\cdot}10$, $\beta\Delta S = 0{\cdot}095$. The uncertainty in h is $\pm 0{\cdot}5$ mm. ○, $\omega = 0$; ▲, $\omega = 1{\cdot}38\,\mathrm{s}^{-1}$.

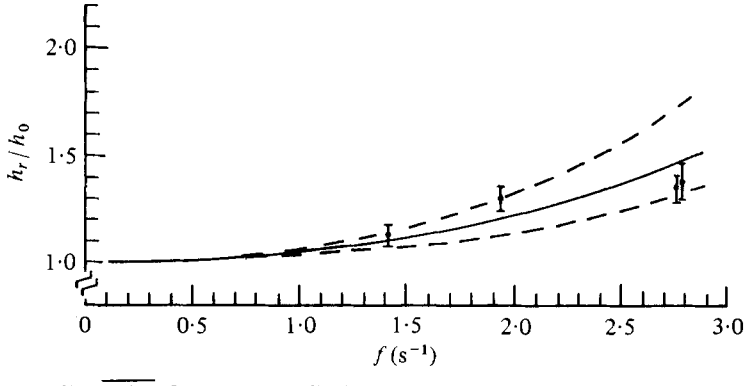

FIGURE 4. The $\overline{h_r/h_0}$ data *vs.* the Coriolis parameter. The solid curve represents F^* with $m = 20{\cdot}4$ cm^{-1}. The dashed curves were calculated at $m = \bar{m} \pm$ the standard deviation.

the values of h_r/h_0 calculated from the $h(t)$ data (figures 2 and 3) at equivalent elapsed times in the rotating and non-rotating runs. (In experiment A 3, where the photographs were not taken at the same intervals as in the non-rotating experiment, a linear fit to the $h_0(t)$ data provided the reference values of h_0 at the appropriate times.) $\overline{h_r/h_0}$ is included in table 1, along with the standard deviation about the mean, and plotted *vs.* the Coriolis parameter in figure 4. Also included are curves derived from the analysis in the next section.

3. Collective instability of rotating salt fingers

In order to refine further and to test the idea that the interface thickness is limited by the collective-instability mechanism [equation (1.1)] we have extended the model of Stern (1969, 1975) to include rotation. Rotation will not affect the purely vertical velocities within the fingers themselves. For small deviations from the vertical, it is appropriate to use the same model of the finger motion as is used in the non-rotating problem; the effects of rotation appear only in the dynamics of the destabilizing perturbation.

We shall follow the notation of Stern (1975, hereafter referred to as II) and work in Cartesian co-ordinates (x, y, z) and not in the tilted system of the wave perturbation as in Stern (1969, hereafter referred to as I). The undisturbed field of fingers is in hydrostatic and diffusive equilibrium, the motion is entirely vertical, and the fields of temperature, salinity and velocity are given by

$$\left.\begin{aligned} T - T_0 &= \bar{T}_z Z + T' \sin lx \sin ly, \\ S - S_0 &= \bar{S}_z Z + S' \sin lx \sin ly, \\ W &= W' \sin lx \sin ly, \end{aligned}\right\} \tag{3.1}$$

where

$$\frac{2\pi}{l} = 2\pi \left[\frac{g}{\nu}\left(\frac{B\bar{S}_z}{K_S} - \frac{\alpha \bar{T}_z}{K_T}\right)\right]^{-\frac{1}{4}} \tag{3.2}$$

is the horizontal wavelength of the fingers, $\bar{T}_z$ and $\bar{S}_z$ are the horizontally averaged vertical gradients of T and S, and the equation of state is assumed linear, i.e.

$$\rho = \rho_0[1 - \alpha(T - T_0) + \beta(S - S_0)], \tag{3.3}$$

in which α and β are the density expansion coefficients for changes in T and S respectively, and ρ_0 is the density at (T_0, S_0). The relations (3.1)–(3.3) satisfy the finite amplitude Boussinesq equations in a fluid unbounded in the vertical and are derived in Lambert & Demenkow (1972) and Huppert & Manins (1973). The time-dependent form is considered in II.

Consider the field of fingers to be perturbed by a large-scale wave with wavelength $2\pi/m$ such that $2\pi/m > 2\pi/l$. The molecular diffusion of T and S may be neglected on this scale, and we parameterize the transport of heat and salt by their averaged finger fluxes:

$$F_T = \overline{WT} = \tfrac{1}{4}W'T', \quad F_S = \overline{WS} = \tfrac{1}{4}W'S'. \tag{3.4}$$

Using the expansion coefficients in (3.3), it is possible to define a net density flux $\beta F_S - \alpha F_T$ and examine its effects on the density perturbation ρ_m due to the wave.

The equation for the conservation of density is written as (equation 11.3.2 of II)

$$\frac{1}{\rho_0}\frac{D\rho}{Dt} = \left(\frac{\partial}{\partial t} + \mathbf{V}_m \cdot \nabla\right)(\rho'_m + \overline{\rho(z)}) = -\nabla \cdot (\beta \mathbf{F}_S - \alpha \mathbf{F}_T). \tag{3.5}$$

In the undisturbed equilibrium model the fluxes would be non-divergent, but we expect that the disturbing wave will produce flux convergence so we must examine the behaviour of the fluxes when acted upon by the infinitesimal perturbation velocity $\mathbf{V}_m$. The flux magnitudes will be regarded as constant in time; only the change in their directions will be considered. The density flux is given by

$$\beta \mathbf{F}_S - \alpha \mathbf{F}_T = -(\beta F_S - \alpha F_T)\,\xi(t),$$

where $\xi(t)$ is a unit vector aligned with the velocity in the salt-finger cells and $\beta F_S - \alpha F_T$ is the magnitude of the density flux. $\xi(t)$ is initially vertical ($\xi(0) = (0, 0, 1)$) and is then tilted from the vertical by the shear of the wave. The horizontal components of $\xi(t)$ grow at a rate proportional to the shear of the wave but the vertical component decreases at a rate that is quadratic in the wave shear. Keeping only the lowest-order terms, we may write the time derivative of $\xi(t)$ as

$$\frac{\partial \xi}{\partial t} \simeq \frac{\partial u_m}{\partial z}\hat{\mathbf{i}} + \frac{\partial v_m}{\partial z}\hat{\mathbf{j}}, \tag{3.6}$$

where $(u_m \hat{\mathbf{i}}, v_m \hat{\mathbf{j}}, w_m \hat{\mathbf{k}}) = \mathbf{V}_m$. The divergence of $\partial \xi / \partial t$ is then

$$\nabla \cdot \frac{\partial \xi}{\partial t} = \frac{\partial}{\partial x}\frac{\partial u_m}{\partial z} + \frac{\partial}{\partial y}\frac{\partial v_m}{\partial z} = \frac{\partial^2 w_m}{\partial z^2} \tag{3.7}$$

by continuity of the perturbation velocity field ($\nabla \cdot \mathbf{V}_m = 0$). The above relation may be used in the time derivative of (3.5) to obtain

$$\frac{1}{\rho_0}\frac{\partial}{\partial t}\left(\frac{\partial}{\partial t} + \mathbf{V}_m \cdot \nabla\right)(\rho'_m + \overline{\rho(z)}) = -(\beta F_S - \alpha F_T)\frac{\partial^2 w_m}{\partial z^2}.$$

When linearized, this becomes

$$\frac{\partial}{\partial t}\left[\frac{\partial}{\partial t}\frac{\rho'_m}{\rho_0} - (\alpha \overline{T}_z - \beta \overline{S}_z)\, w_m\right] = -(\beta F_S - \alpha F_T)\frac{\partial^2 w_m}{\partial z^2} \tag{3.8}$$

(equation 11.3.5 of II).

The equations of motion for the perturbation are the linearized Boussinesq equations in a rotating co-ordinate system:

$$(\partial/\partial t - \nu \nabla^2)\,\mathbf{V}_m + f\hat{\mathbf{k}} \times \mathbf{V}_m = -\nabla \phi_m - g\hat{\mathbf{k}}\rho'_m/\rho_0, \tag{3.9}$$

where $f = 2\omega$ is the Coriolis parameter and viscosity is retained as the dissipative mechanism for the wave. ϕ_m represents the pressure perturbation due to the wave:

$$\phi_m = \frac{P}{\rho_0} - \frac{1}{\rho_0}\int_0^z \overline{\rho(z)}\, g\, dz - r^2\omega^2.$$

The momentum equations for $\mathbf{V}_m$ should contain Reynolds-stress terms due to the vertical motion in the smaller-scale fingers but we shall neglect these as they are small compared with the buoyancy and viscous stresses. This was justified in I by an estimate of the salt-finger Reynolds number, which was of order 1.

The component equations are

$$(\partial/\partial t - \nu\nabla^2)\, u_m - f v_m = -\partial\phi_m/\partial x,$$
$$(\partial/\partial t - \nu\nabla^2)\, v_m + f u_m = -\partial\phi_m/\partial y,$$
$$(\partial/\partial t - \nu\nabla^2)\, w_m = -\partial\phi_m/\partial z - g\rho'_m/\rho_0.$$

These may be combined with the continuity relation to yield

$$\left(\frac{\partial}{\partial t} - \nu\nabla^2\right)^2 \nabla^2 w_m + f^2 \frac{\partial^2 w_m}{\partial z^2} + \left(\frac{\partial}{\partial t} - \nu\nabla^2\right)^2 \nabla_h^2 g \frac{\rho'_m}{\rho_0} = 0, \tag{3.10}$$

where $\nabla_h^2 = \partial^2/\partial x^2 + \partial^2/\partial y^2$. When (3.8) is used to eliminate ρ'_m we obtain

$$\left(\frac{\partial}{\partial t} - \nu\nabla^2\right)^2 \nabla^2 \frac{\partial^2 w_m}{\partial t^2} + g(\alpha\overline{T}_z - \beta\overline{S}_z)\left(\frac{\partial}{\partial t} - \nu\nabla^2\right)\nabla_h^2 \frac{\partial w_m}{\partial t}$$
$$+ \left(f^2 \frac{\partial^2}{\partial t^2} - g(\beta F_S - \alpha F_T)\left(\frac{\partial}{\partial t} - \nu\nabla^2\right)\nabla_h^2\right) \frac{\partial^2 w_m}{\partial z^2} = 0. \tag{3.11}$$

This is a complete linear equation for w_m.

We can now examine the plane-wave solutions to (3.11) appropriate for an unbounded fluid. There is no loss of generality if we orient the wave (phase) vector completely in the x, z plane. The solutions take the form

$$w_m \approx \exp\{\Omega t + im(x\sin\theta + z\cos\theta)\}, \tag{3.12}$$

where Ω is the complex growth rate, $2\pi/m$ is the wavelength and θ is the angle between the wave vector and the vertical. By substituting (3.12) into (3.11) we find that the growth rate must satisfy the quartic relation

$$(\Omega + \nu m^2)\,[(\Omega + \nu m^2)\,\Omega^2 + g(\alpha\overline{T}_z + \beta\overline{S}_z)\sin^2\theta\,\Omega$$
$$+ g(\beta F_S - \alpha F_T)\sin^2\theta\cos^2\theta\, m^2] + f^2\cos^2\theta\,\Omega^2 = 0. \tag{3.13}$$

We wish to determine the conditions for neutral stability, when the real part of Ω is zero. Substituting a pure imaginary growth rate (frequency) $\Omega = i\Omega'$ into (3.13) yields two equations in Ω':

$$\Omega'^4 - [g(\alpha\overline{T}_z - \beta\overline{S}_z)\sin^2\theta + f^2\cos^2\theta + \nu^2 m^4]\,\Omega'^2$$
$$+ \nu m^4 g(\beta F_S - \alpha F_T)\sin^2\theta\cos^2\theta = 0, \tag{3.14a}$$

$$-2\nu m^2\Omega'^3 + [\nu m^2 g(\alpha\overline{T}_z - \beta\overline{S}_z)\sin^2\theta$$
$$+ m^2 g(\beta F_S - \alpha F_T)\sin^2\theta\cos^2\theta]\,\Omega' = 0. \tag{3.14b}$$

The non-trivial root of (3.14b) is

$$\Omega'^2 = \tfrac{1}{2}\sin^2\theta\,(g(\alpha T_z - \beta S_z) + (g/\nu)\,(\beta F_S - \alpha F_T)\cos^2\theta]. \tag{3.15}$$

Insertion of this expression in (3.14a) yields a relationship which must be satisfied at the point of neutral stability:

$$\tfrac{1}{4}\sin^2\theta\,[g(\alpha\overline{T}_z - \beta\overline{S}_z) + (g/\nu)\,(\beta F_S - \alpha F_T)\cos^2\theta]^2 - \tfrac{1}{2}[g(\alpha\overline{T}_z - \beta\overline{S}_z)\sin^2\theta + f^2\cos^2\theta + \nu^2 m^4]$$
$$\times\,[g(\alpha\overline{T}_z - \beta\overline{S}_z) + (g/\nu)\,(\beta F_S - \alpha F_T)\cos^2\theta] + \nu^2 m^4 (g/\nu)\,(\beta F_S - \alpha F_T)\cos^2\theta = 0. \tag{3.16}$$

This expression can also be obtained by requiring that, for the roots $\Omega = \pm i\Omega'$ [given by (3.15)], the expression

$$\Omega^2 + \tfrac{1}{2}\sin^2\theta[g(\alpha\bar{T}_z - \beta\bar{S}_z) + (g/\nu)(\beta F_S - \alpha F_T)\cos^2\theta]$$

be a factor of (3.13). That is, performing the polynomial division and setting the remainder equal to zero yields (3.16).

Besides the appearance of the Coriolis parameter, there is a major difference between the relation (3.16) and that of Stern (I, II); the criterion for the instability of rotating salt fingers is dependent on the wavenumber of the perturbation, whereas the non-rotating criterion is independent of the wavenumber. We also find that there is a different dependence on θ.

To investigate (3.16) we cast it in a non-dimensional form, using the following substitutions:

$$F = \frac{(\beta F_S - \alpha F_T)}{\nu(\alpha\bar{T}_z - \beta\bar{S}_z)}, \quad R = \frac{f^2}{g(\alpha\bar{T}_z - \beta\bar{S}_z)} = \frac{f^2}{N^2},$$

$$M = m\left(\frac{\nu^2}{g(\alpha\bar{T}_z - \beta\bar{S}_z)}\right)^{\frac{1}{4}}, \quad X = \cos^2\theta.$$

We can then express (3.16) as a quadratic in F:

$$(X^2 - X^3)F^2 + 2X(M^4 - RX)F + X(1-2R) - 2M^4 - 1 = 0. \tag{3.17}$$

F is the ratio of the density flux to the density gradient (scaled with the viscosity) which appeared in the non-rotating stability problem, R is the square of the ratio of the inertial frequency to the Brunt–Väisälä frequency N; M is the dimensionless wavenumber magnitude, and X contains the dependence on the angle of inclination of the wavenumber vector to the vertical. In I and II it was found that $F = X^{-1}$, giving a minimum critical flux of $F = 1$ when $\theta \to 0$. This means that the wave vector is vertical and there is a steady horizontal drift as $\Omega \to 0$ ($\Omega^2 = N^2\sin^2\theta$, $\theta \to 0$). We expect some constraints on such motion in the rotating frame, however, and we must investigate the two roots of (3.17). These are given by

$$F = \{RX - M^4 \pm [(M^4+1)^2 + X^2(R-1)^2 + 2X(R - M^4 - RM^4 - 1)]^{\frac{1}{2}}\}/(X - X^2). \tag{3.18}$$

Examining (3.18) when $R = 0$ (no rotation), we find that the 'negative' root yields a negative quantity, $F = [-2M^4 - (1-X)]/(X - X^2)$. This is physically impossible for the salt-finger case, since energetics require that $\beta F_S - \alpha F_T > 0$ and

$$\alpha\bar{T}_z - \beta\bar{S}_z = -\rho_0^{-1}\,\partial\bar{\rho}/\partial z > 0$$

for gravitational stability. The 'positive' root, however, does reduce to $F = X^{-1}$ as in I and II; thus all further work is done with this root. We also require that F be real, or that the quantity

$$B \equiv (M^4+1)^2 + X^2(R-1)^2 + 2X(R - M^4 - RM^4 - 1)$$

be non-negative. Since $1 \geqslant X \geqslant 0$, $R \geqslant 0$ and $M^4 \geqslant 0$ this is always satisfied; the minimum value of B is zero, when $R = M^4 = X = 1$.

We can now compute $F = (RX - M^4 + B^{\frac{1}{2}})/(X - X^2)$ for different values of the parameters. In figure 5, F is plotted *vs.* X for various R and M. F has a minimum with respect to X at some value of $X < 1$ for all $R > 0$. We also note that for large

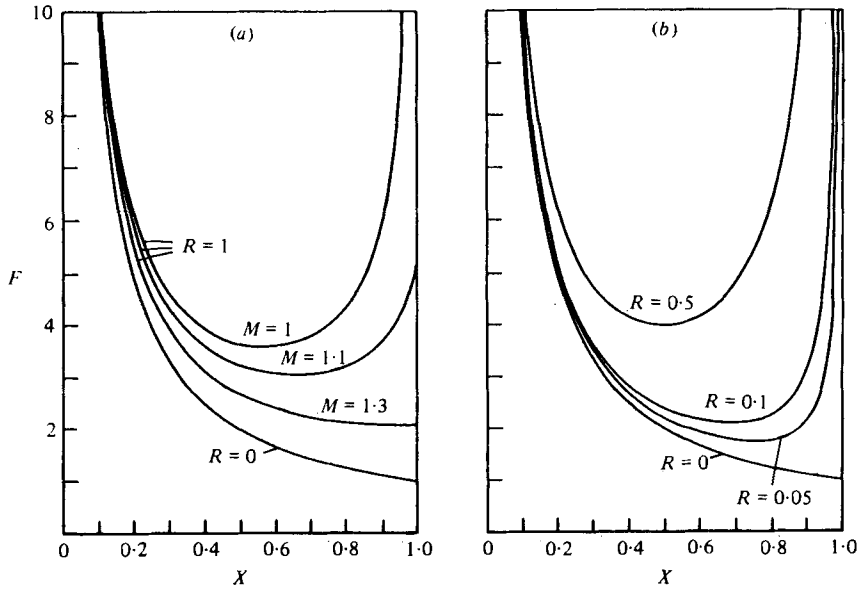

FIGURE 5. (*a*) F *vs.* X for $R = 1$ and various M. The non-rotating case ($R = 0$) $F = X^{-1}$ is also shown. The value of X at the minimum of F approaches 1 as M increases. (*b*) F *vs.* X for $M = 0$ and various R.

values of the wavenumber ($M^4 > R$) the effects of rotation become negligible; the curves approach the curve $F = X^{-1}$ appropriate for non-rotating fingers, and the least stable flux occurs at values of X closer to 1 (smaller angles from the vertical).

Since the analysis assumed only infinitesimal perturbation amplitudes, we expect that the first 'waves' to grow (and potentially dominate the fully developed turbulent regime) will be those with the lowest value of the critical flux. F can be minimized with respect to X by solving

$$\frac{dF}{dX} = \frac{(X-X^2)(R+\frac{1}{2}B^{-\frac{1}{2}}B') - (1-2X)(RX-M^4+B^{\frac{1}{2}})}{(X-X^2)^2} = 0, \tag{3.19}$$

where $B' = dB/dX = 2X(R-1)^2 + 2(R-M^4-RM^4-1)$. The root of (3.19) (designated by $X_{\min}$) was found numerically, using an iterative technique, for various R and M. The minimum critical flux was then plotted *vs.* the wavenumber M for several rotation rates R (figure 6). As in figure 5, it is apparent that for large enough wavenumbers ($M^4 > R$) rotation has only a slight stabilizing effect. The value of $X_{\min}$ approaches 1 in this limit, and setting $X = 1$ in (3.17) allows us to write

$$F^* = \frac{M^4+R}{M^4-R} = \frac{\nu^2 m^4 + f^2}{\nu^2 m^4 - f^2}. \tag{3.20}$$

F^* is an approximate form of the neutral curve valid for dimensional wavenumbers greater than an 'Ekman' wavenumber $(f/\nu)^{\frac{1}{2}}$. The relation of F^* to F is shown in figure 7. This approximation is helpful to the understanding of the problem. Small-scale waves will be only slightly affected by rotation because of large viscous stresses. Larger size (small m) perturbations are less affected by viscosity because of their lower shears and so feel the stabilizing effects of rotation. A laminar 'Ekman depth'

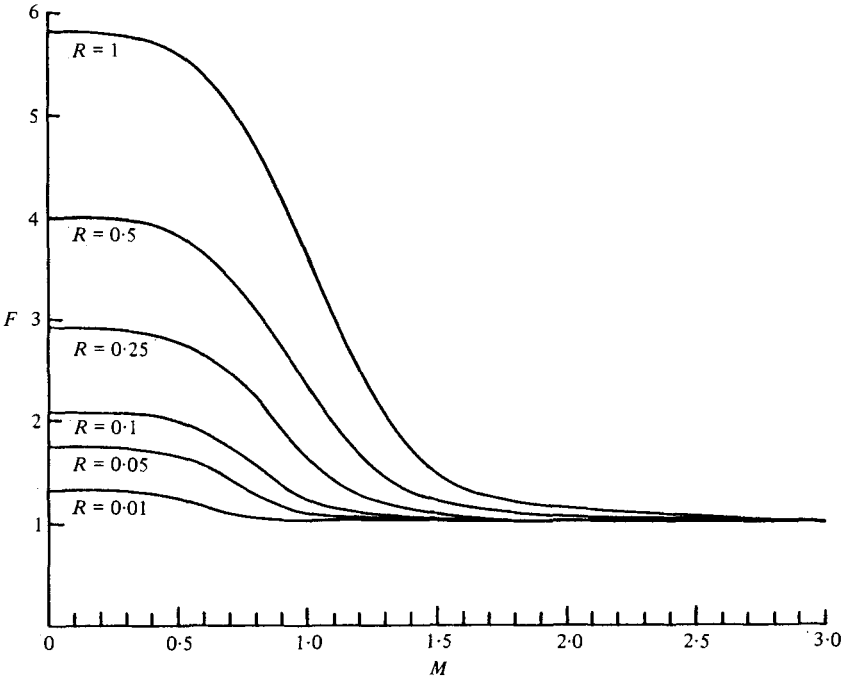

FIGURE 6. F as a function of M for various R and $X = X_{\min}$, the root of $dF/dX = 0$.

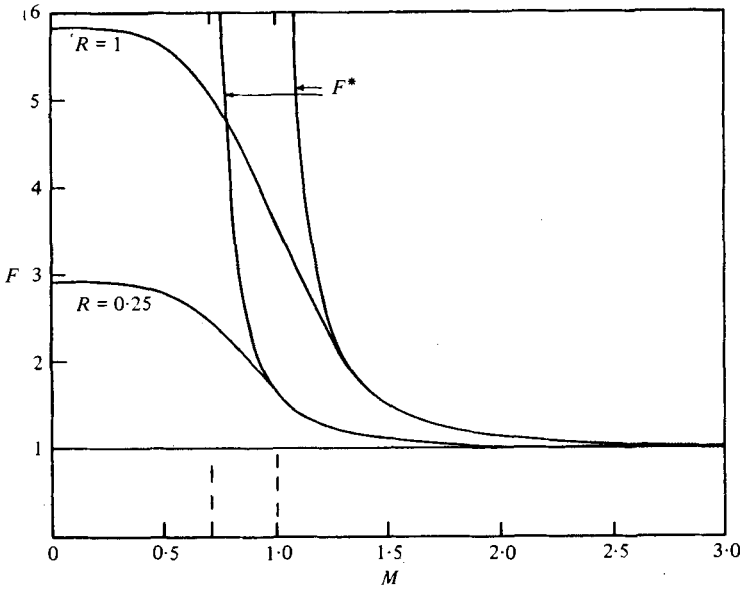

FIGURE 7. The relation of F^* to F. The vertical lines indicate where $M = R^{\frac{1}{4}}$ and the dimensional wavenumber m is equal to $(\nu/f)^{\frac{1}{4}}$.

$2\pi(\nu/f)^{\frac{1}{2}}$ is the appropriate length scale that distinguishes between a large or small stabilization due to Coriolis accelerations.

Since the lowest critical flux is found for $M^4 > R$, we might expect small-scale instabilities to dominate the breakdown process. There is a limit on the smallness of the disturbances imposed by the salt-finger width, however. That is, the theory is not expected to apply when m exceeds l, the finger wavenumber. This limit is expressed as

$$m_c = \left[\frac{g}{\nu}\left(\frac{\beta\bar{S}_z}{K_S} - \frac{\alpha\bar{T}_z}{K_T}\right)\right]^{\frac{1}{4}},$$

or in terms of the dimensionless wavenumber,

$$M_c = \left(\frac{\nu}{K_T}\right)^{\frac{1}{4}} \left(\frac{\frac{K_T}{K_S}\frac{\beta\bar{S}_z}{\alpha\bar{T}_z} - 1}{1 - \frac{\beta\bar{S}_z}{\alpha\bar{T}_z}}\right)^{\frac{1}{4}}.$$

The second factor on the right is generally of order unity so we expect the upper limit on the dimensionless wavenumber to be the $\frac{1}{4}$ power of the Prandtl number for heat–salt fingers and the $\frac{1}{4}$ power of the Schmidt number for sugar–salt fingers. We do not expect the theory to hold for dimensionless wavenumbers greater than M_c.

4. Discussion

The analysis in the preceding section may be related to the experimental results in the following manner. Using a finite-difference approximation

$$F \sim (\beta F_S - F_T)_r h_r / \nu(\alpha\Delta T - \beta\Delta S)_r$$

to the collective-instability condition for the rotating system and using (2.1) for the non-rotating system, we may write

$$\frac{h_r}{h_0} \simeq \frac{(\beta F_S}{(\beta F_S} \frac{\alpha F_T)_0 (\alpha\Delta T - \beta\Delta S)_r}{-\alpha F_T)_r \alpha\Delta T - \beta\Delta S)_0} F(R, M). \tag{4.1}$$

Since we have assumed the fluxes to be unchanged by rotation for equal initial values of $\alpha\Delta T$ and $\beta\Delta S$, this reduces to

$$h_r/h_0 \simeq F(R, M). \tag{4.2}$$

Direct measurements of the density difference across the interface were not made. We can, however, make rough estimates for R for the case $\beta\Delta S = 0{\cdot}090$, using data from Lambert & Demenkow (1972). A finite-difference estimate can be expressed as $R \simeq f^2 h_r / g(\alpha\Delta T - \beta\Delta S)$. The quantity $\alpha\Delta T - \beta\Delta S$ increases rather slowly compared with h_r, so R varies nearly as much as h_r during the course of an experiment. Using h_r/h_0 to approximate F and the density data of Lambert & Demenkow (1972) to calculate R, we can find a value of M, the non-dimensional wavenumber of the instability, that satisfies $h_r/h_0 = F(R, M)$ [(3.18) with the plus sign and with $X = X_{\min}$] for each estimate of h_r/h_0. The value of M is also found to vary between the beginning and the end of each experiment. R varies from 0·08 to 1·3 and M from 0·9 to 1·8 with M always greater than R. The ranges of these estimates for R and M are included in table 2.

Experiment	f (s^{-1})	$\overline{h_r/h_0}$	R	M	$\bar{m}$ (cm^{-1})
$B2$	1·414	1·14	0·08–0·34	1·0–1·5	19·6 ± 1·8
$A3$	1·932	1·30	0·11–0·64	0·9–1·5	18·8 ± 0·8
$B3$	2·763	1·35	0·29–1·30	1·2–1·8	21·7 ± 0·9
$C2$	2·763	1·39	—	—	20·9 ± 0·9

TABLE 2. The estimated ranges of R and M for the experiments. No density data were available for $C1$ and $C2$; thus no estimate of R could be made. $\bar{m}$ is the average of the values of m calculated from (3.20) for each h_r/h_0. The viscosity was taken to be $\nu = 1{\cdot}53 \times 10^{-2}$ cm^2 s^{-1} for $\beta\Delta S = 0{\cdot}09$ and $\nu = 1{\cdot}58 \times 10^{-2}$ cm^2 s^{-1} for $\beta\Delta S = 0{\cdot}095$.

Since $M^4 > R$ we can apply the approximation $h_r/h_0 \simeq F^* = (\nu^2 m^4 + f^2)/(\nu^2 m^4 - f^2)$ [see (3.20)], in which the stratification no longer appears, and calculate the *dimensional* wavenumber m for each experiment. In contrast to the variation of R and M, m remains relatively constant for each run and changes little between the different experiments. Average values of m and the standard deviations are included in table 2. The mean of the data from all experiments is $\bar{m} = 20{\cdot}4 \pm 1{\cdot}6$ cm^{-1}. Curves of (3.20) using $\bar{m}$ and $\bar{m} \pm$ standard deviation are shown in relation to the h_r/h_0 data in figure 4.

The significance of this constant wavenumber is not clear, but some speculation is possible. Recall that, in the approximation of (3.20), $\theta \simeq 0$, i.e. m is directed vertically. We might interpret $2\pi/m$ as a vertical distance over which the collective-instability mechanism acts. If we assume the interior of a finger interface to be marginally stable and the edges, where the breakdown occurs, to be critical or slightly supercritical with respect to collective instability, then the vertical length scale of 3·1 mm (which is less than an Ekman thickness and greater than the finger width, ~ 1 mm) may correspond to the thickness of the edge transition zones. The thickness of these transition zones, where the salt fingers give way to convective turbulence, certainly appears to be of this order in the photographs (see figure 8, plate 2).

This interpretation is meant as only a speculation, the application of this linear theory to the highly supercritical conditions of these two-layer run-down experiments cannot be rigorously justified. Also the estimated wavelength of instability is uncomfortably close to the finger width, and diffusion effects neglected in the model might be important on this scale. We do feel, however, that the data are at least qualitatively consistent with the collective-instability model.

At any rate it is not clear how one could otherwise explain the observed increase in interface thickness in these strongly rotating experiments. The Taylor number f^2H^4/ν^2, a measure of the relative effects of rotation and viscosity, is of order 10^8 and the Rossby number W/fH, the ratio of inertial to rotational effects, is less than one when typical convection velocities (a few mm/s) in the mixed layers are used. One might have expected the inhibition of finger convection under these conditions, because rotation delays the onset of convection in the rotating Rayleigh problem (Chandrasekhar 1961, chap. III) and also inhibits the growth of finger modes in the linear stability analysis of Pearlstein (1976). But the present experiments were highly supercritical with respect to the formation of salt fingers and the fingers were removed from solid horizontal boundaries, which are probably essential to the inhibiting effects of rotation in the above-mentioned studies. Our view is that the interface thickness is internally controlled and independent of the mixed-layer depths; this is

also supported by the experiments of Demenkow (1973). The collective-instability model is the only available model which addresses the problem of the finger interface thickness. Including rotation in the model yields results consistent with those observed experimentally.

5. Summary and conclusions

We have demonstrated in laboratory experiments with two-layer sugar–salt fingers that the effect of rotation on a fingering interface is to cause it to thicken more rapidly than it does in an inertial frame of reference. Also, the degree of order in the horizontal structure appears to be reduced by rotation. These results are interpreted as being due to stabilization of the fingers by the rotation, and are consistent with an extension of the collective-instability model of Stern (1969, 1975) to a rotating frame. The added constraint of rotation allows the calculation of the wavenumber of the instability when the interface thickness data are used in an expression [equation (3.20)] derived from the theory. This wavenumber, which is found to remain relatively constant (within 10 %) for three rotation rates and two different stratifications, is interpreted as corresponding to a vertical length scale over which the collective-instability mechanism acts. The length scale compares well with the thickness of the observed transition regions between the laminar salt fingers in the interior of the interface and the fully developed turbulence in the mixed layers above and below. The lower degree of order among the fingers may be a consequence of the spiral velocity structure of the inertial–gravity wave perturbations examined in the model. While these experiments do not *prove* the validity of the collective-instability theory, they are at least qualitatively consistent with the model and increase our confidence in its use in salt-finger flux models (Stern 1976).

The authors wish to thank Dr Melvin E. Stern for many helpful discussions during the course of this study. This work was supported by the Oceanography Section of the National Science Foundation, Grant no. OCE-75-14113-A02.

REFERENCES

CHANDRASEKHAR, S. 1961 *Hydrodynamic and Hydromagnetic Stability*. Oxford: Clarendon Press.

DEMENKOW, J. W. 1973 A study of the two layer salt finger system. Ph.D. dissertation, University of Rhode Island.

HUPPERT, H. E. & MANINS, P. C. 1973 Limiting conditions for salt-fingering at an interface. *Deep-Sea Res.* **20**, 315–323.

LAMBERT, R. B. & DEMENKOW, J. W. 1972 On the vertical transport due to fingers in double-diffusive convection. *J. Fluid Mech.* **54**, 627–640.

LAMBERT, R. B. & STURGES, W. E. 1977 A thermohaline staircase and vertical mixing in the thermocline. *Deep-Sea Res.* **24**, 211–222.

LINDEN, P. F. 1973 On the structure of salt fingers. *Deep-Sea Res.* **20**, 325–340.

PEARLSTEIN, A. J. 1976 Effect of rotation on the stability of a doubly diffusive fluid layer. *Inst. Geophys. Planetary Phys., Univ. Calif., Los Angeles*, publ. 1636.

SHIRTCLIFFE, T. G. L. & TURNER, J. S. 1970 Observations of the cell structure of salt fingers. *J. Fluid Mech.* **41**, 707–720.

STERN, M. E. 1960 The 'salt-fountain' and thermohaline convection. *Tellus* **12**, 172–175.

STERN, M. E. 1969 Collective instability of salt fingers. *J. Fluid Mech.* **25**, 209–218.

STERN, M. E. 1975 *Ocean Circulation Physics*. Academic Press.

STERN, M. E. 1976 Maximum buoyancy flux across a salt finger interface. *J. Mar. Res.* **34**, 95–110.

STERN, M. E. & TURNER, J. S. 1969 Salt fingers and convecting layers. *Deep-Sea Res.* **16**, 497–511.

TAIT, R. I. & HOWE, M. R. 1968 Some observations of thermohaline stratification in the deep ocean. *Deep-Sea Res.* **15**, 275–280.

TURNER, J. S. 1967 Salt fingers across a density interface. *Deep-Sea Res.* **14**, 599–611.

TURNER, J. S. & CHEN, C. F. 1974 Two-dimensional effects in double-diffusive convection. *J. Fluid Mech.* **63**, 577–592.

WILLIAMS, A. J. 1975 Images of ocean microstructure. *Deep-Sea Res.* **22**, 811–829.

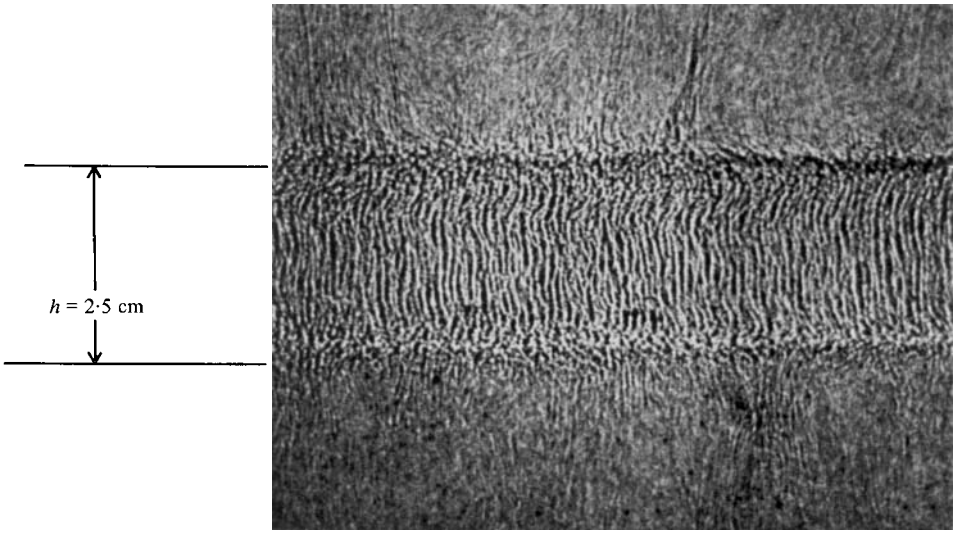

(*a*)

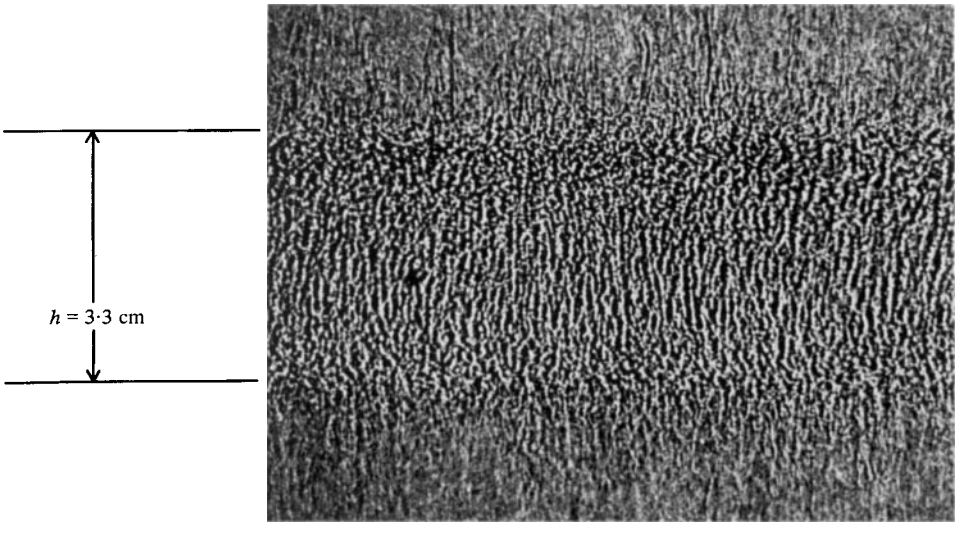

(*b*)

FIGURE 1. Photographs of the fingering interface for experiments with $\alpha\Delta T = 0{\cdot}10$, $\beta\Delta S = 0{\cdot}09$ at $t = 600$ min. (*a*) Non-rotating, $\omega = 0$. (*b*) Rotating, $\omega = 1{\cdot}38\,\mathrm{s}^{-1}$. The rotating interface is thicker than the non-rotating interface and the fingers show less vertical alignment.

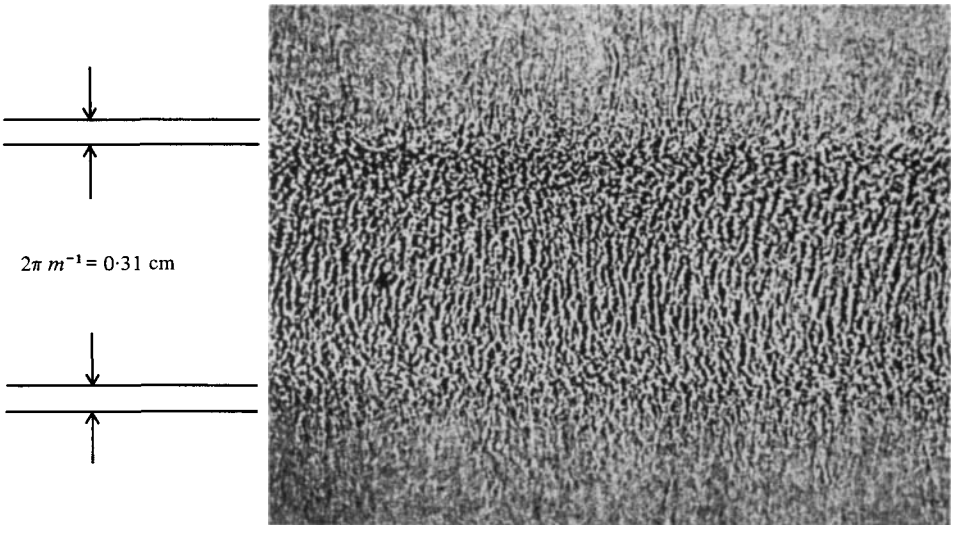

FIGURE 8. Photograph of the rotating interface with the length scale obtained from the theory (0·31 cm) compared with the thickness of the edge transition regions. $\alpha\Delta T = 0{\cdot}10$, $\beta\Delta S = 0{\cdot}09$, $\omega = 1{\cdot}38\,\mathrm{s}^{-1}$, $t = 600$ min.